Peer-reviewed version available at Energies 2018, 11, 2857; doi:10.3390/en11102857

Article

A Study about performance and robustness of model predictive controllers in WECs systems

Rafael Guardeño [1], Agustín Consegliere [1] and Manuel J. López [1]

[1] Escuela Superior de Ingeniería, Universidad de Cádiz, Puerto Real 11519, España; rafael.guardeno@uca.es; agustin.consegliere@uca.es; manueljesus.lopez@uca.es

Abstract: This work is located in a growing sector within the field of renewable energies, wave energy converters (WECs). Specifically, it focuses on one of the point absorbers wave (PAWs) of the hybrid platform W2POWER. With the aim of maximising the mechanical power extracted from the waves by these WECs and reduce their mechanical fatigue, the design of five different model predictive controllers (MPCs) with hard and soft constraints has been carried out. As contribution of this paper, two of the MPCs have been designed with the addition of an embedded integrator. In order to validate the MPCs, an exhaustive study on performance and robustness is realized through simulations carried out in which uncertainties in the WEC dynamics are considered. Furthermore, looking for realistic in these simulations, an identification methodology for PAWs is proposed and validated by means of real time series of a scale prototype.

Keywords: wave energy converter; model predictive control; comparitive of robustness; embedded integrator; mathematical model; identification methodology; real time series

1. Introduction

Nowadays, the main motivation for the research and development of wave energy converters (WECs) are the advantages offered by waves: a clean and abundant energy. As evidence, the authors in [1] compare a global study of net wave power (estimated at about 3 TW) with the electrical power consumed globally in 2008 (equivalent to an average power of 2.3 TW). However, it should be noted that currently there isn't clear line of development, but a great diversity of systems based on different approaches to extract energy from the waves. In particular, the ocean energy systems collaboration programme [2] classifies three kinds of WEC systems: oscillating water columns, overtopping and wave activated bodies (WABs). This work focuses on a type of WAB systems, a point absorber wave (PAW) energy converter from W2POWER platform [3]. These systems are characterized because their extension is significantly smaller than the predominant wave wavelengths. In addition, PAWs extract the maximum mechanical power from the sea when they are in resonance with the excitation force caused by the waves [29]. In order to favour this situation, it is necessary to enlarge the bandwidth of these devices. For this reason several control systems are used, the most common are: Passive Loading Control, Reactive Loading Control and Latching Control [5,6]. Although, since the last decade, more complex controllers as the MPC (Model Predictive Control) are being employed. The interest in implementing MPCs in WECs systems is motivated by the need to increase the productive/economic viability of these systems. Because these controllers allow to minimize mechanical fatigue in the devices (limiting the operating ranges) and to focus the control strategy directly to the maximization of the extracted power.

Actually, several authors have developed predictive controllers for WECs [7–17]. These MPCs controllers can be grouped according to the characteristics of the cost function optimized. On the one hand, the authors in [8,10–16] use a cost function in which the extraction of mechanical power is directly maximized. Whereas, on the other hand, in [9,17] the authors propose a cost function to maximise power extraction by minimising the error between the speed of oscillation of the system and a setpoint for it. In addition to the above classification, MPC controllers can be distinguished

according to the mathematical model used for their design. On one side, in [9–11,13,14] a reduced model is used for the design, which does not consider the dynamics of the radiation force. Meanwhile, in [7,8,12,13,15–17] such dynamics are considered in the design model. Moreover, the previous works do not consider the dynamics of the power take-off system (PTO) neither in the evaluation nor in the design of the MPCs. In this aspect the authors in [11,14], although they do not consider the dynamics of the PTO, optimize the cost function for the increment of the control signal, thus limiting the slew rate of the actuator. Finally, it should be highlighted the treatment carried out in the case of non-feasibility when solving the cost functions with restrictions that define the MPCs. In this aspect, the works carried out in [9,10,13] considers a more complete approach by adding soft constrains in case of non-feasibility.

This paper analyses the main approaches of MPCs applied to PWAs systems [8–17]. In addition, a new design is proposed: MPC based on a model with embedded integrator for controllers that follow a setpoint for the velocity of oscillation of the PWA. This approach is recommended in the theory of predictive control in the space of states [18,19] and it is opposite of the one used in [9,17] for PAWs systems. Moreover, all predictive controllers of this work consider soft and hard constraints. On the other hand, the dynamics of the PTO is taken into account to validate the MPCs controllers, as well as in the design of some of these controllers. After an exhaustive fine-tuning for all MPCs, the mains contributions of this work are obtained, in-depth study about performance and robustness of all MPCs through simulations carried out. Furthermore, looking for the realistic in these comparitives, an identification methodology for PAWs is proposed and validated by means of real time series of a scale prototype.

The rest of the article is organized as follows: Section 2 presents the generic mathematical model of a PAW, the identification methodology proposed in this paper and the treatment applied to the model identified for its later use in the design of the MPCs. Section 3 details the five MPC controllers designed with hard and soft restrictions; while section 4 presents the results obtained by applying the five MPCs to the identified model and two comparisons of the MPCs; one of their closed-loop behaviour and the other of their robustness. Finally, in section 5, the main conclusions are indicated.

2. Mathematical model

Given the importance of mathematical modeling in the design of MPC controllers, this section begins by describing the generic model of a PAW. This is followed by the identification process proposed in this paper for the study system, one of the WECs systems of the platform W2POWER [3]. Later, the treatment of the model is detailed for its later use in the design of MPC controllers.

2.1. Generic mathematical model for point absorver wave

The modeling of the forces affecting a PAW that extracts power from the waves using a single degree of freedom (*heave*) is widely used in the bibliography [7–9,20–25,29]. The main dynamic interactions between the buoy and the waves are collected by:

$$m\ddot{z} = F_e + F_r + F_s + F_u \tag{1}$$

where m is the mass of the system, z the vertical displacement of the buoy, F_e the excitation force caused by the wave, F_r the radiation force, F_s the hydrostatic restoring force and F_u the control force realized by the PTO system.

The *force of radiation* is due to the effect produced on the system by the waves it radiates when oscillating. It is modeled by Cummins equation [26] as (2), where the radiation force F_r is composed of two terms: Fr_{m_∞} and Fr_{K_r}. The first is a function of the acceleration of the system and the mass of water added m_∞. While the second defines a radiation force in function of the velocity of oscillation as an integral of convolution.

$$F_r = \underbrace{-m_\infty \ddot{w}(t)}_{Fr_{m_\infty}} - \underbrace{\int_\infty^t h_r(t-\tau)w(\tau)d\tau}_{Fr_{K_r}} \tag{2}$$

The term convolution represents the impulse response that relates the velocity of oscillation of the system with the force of radiation. To avoid convolution calculations, an approximation is made based on ordinary differential equations (ODE), or as a transfer function in the Laplace domain (3).

$$\frac{Fr_{K_r}(s)}{W(s)} = K_r(s) = \frac{a_n s^n + a_{n-1}s^{n-1} + \ldots + a_0}{b_n s^n + b_{n-1}s^{n-1} + \ldots + b_0} \tag{3}$$

The *hydrostatic restoring force* represents the effect of Archimedes and gravity on the buoy (4). By linearizing Equation (4), the hydrostatic force is approximated as (5).

$$F_{res} = -(V_{desp}(z)\rho g - mg) \tag{4}$$

$$\begin{aligned} F_{res} &= -k_{res}z(t) \\ k_{res} &= \rho g A_W \end{aligned} \tag{5}$$

where V_{desp} is the volume of water displaced, ρ is the density of seawater, g is the gravity constant, k_{res} is the hydrostatic restoring coefficient and A_W is the area of the buoy on its waterline.

For the *excitation force* caused by the waves, the components with the highest frequency are negligible. For this reason, authors as [7,8,11,12,15,16,22–25] define the excitation force as a low pass filter of first/second order at wave height (6).

$$G_{Fe}(s) = \frac{Fe(s)}{\eta(s)} = \frac{K_\tau}{s^2 + 2\zeta_\tau \omega_{n\tau} s + \omega_{n\tau}^2}. \tag{6}$$

On the other hand, in order to modeling the force on a buoy, it can be used the Morison equation [31], which is habitually employed to estimate the wave loads in the design of offshore structures. By linearizing the Morison equation for point absorver wave in heave, the excitation force is defined according to:

$$F_e(t) = m_\infty \ddot{\eta}(t) + B_{aprox}\dot{\eta}(t) + k_{res}\eta(t) \tag{7}$$

where η is the height of the incoming wave and B_{aprox} represents the damping of the system, which can be obtained as the stationary gain of (3).

The *PTO dynamics* can be approximated as a linear second order system with a force limitation. The linear relation between the demanded force by the control system, (F_u), and the force applied to the buoy, (F_{pto}), is given by (8).

$$G_{pto}(s) = \frac{F_{pto}(s)}{F_u(s)} = \frac{d_a {\omega_n}^2}{s^2 + 2\zeta\omega_n s + {\omega_n}^2}, \tag{8}$$

2.2. Identification methodology for points absorbers wave

In order to increase the realistic of this work, the identification of one of the PAWs of the platform W2POWER (cylindrical buoy: 11 m of length and 7.5 m of diameter) has been carried out. In addition, in the aim of validating the proposed identification methodology, time series of a scale real prototype (obtained in a hydrodynamic experience channel by [27]) have been used.

Preprints (www.preprints.org) | NOT PEER-REVIEWED | Posted: 28 September 2018 doi:10.20944/preprints201809.0556.v1

Peer-reviewed version available at Energies 2018, 11, 2857; doi:10.3390/en11102857

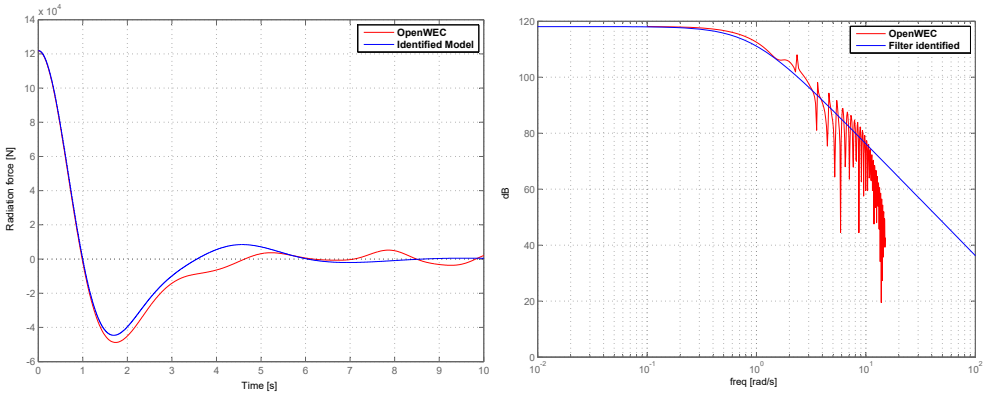

Figure 1. Comparative of the identified transfer functions: (a) Impulse response for radiation force $K_r(s)$. (b) Bode diagram for excitation force $F_e(s)$.

To identify the WAP system, the openWEC software has been used [28]. Among other data, it returns: the added water mass ($m_\infty = 167700$ kg), the impulse response of the radiation force as a function of the oscillation velocity and the frequency response of the excitation force. From these data, the transfer function (9) is identified for the impulse response of the radiation force using the Prony approximation [30]. On the other hand, the low-pass filter that defines the dynamics of the excitation force caused by the incoming wave is tuned to the transfer function (10). The Figure 1 compares the two transfer functions identified with the data delivered by the openWEC software. Finally, the hydrostatic restoring coefficient $k_{res} = 809325[N/m]$ is obtained using the Equation (5).

$$K_r(s) = \frac{F_r(s)}{W(s)} = \frac{a_{K_8}s^8 + a_{K_7}s^7 + a_{K_6}s^6 + a_{K_5}s^5 + a_{K_4}s^4 + a_{K_3}s^3 + a_{K_2}s^2 + a_{K_1}s + a_{K_0}}{s^8 + b_{K_7}s^7 + b_{K_6}s^6 + b_{K_5}s^5 + b_{K_4}s^4 + b_{K_3}s^3 + b_{K_2}s^2 + b_{K_1}s + b_{K_0}} \quad \left[\frac{N}{m/s}\right] \tag{9}$$

where the coefficients a_K and b_K are listed in the Table 1.

$$\frac{F_e(s)}{\eta(s)} = \frac{6.5 \times 10^5}{(s+0.9)^2} \quad \left[\frac{N}{m}\right] \tag{10}$$

Then, regrouping terms according to Equation (1), the transfer function (11) that relates external forces with the position of the buoy (z) is obtained.

$$G_{WEC}(s) = \frac{Z(s)}{F_{ext}(s)} = \frac{a_8s^8 + a_7s^7 + a_6s^6 + a_5s^5 + a_4s^4 + a_3s^3 + a_2s^2 + a_1s + a_0}{s^{10} + b_9s^9 + b_8s^8 + b_7s^7 + b_6s^6 + b_5s^5 + b_4s^4 + b_3s^3 + b_2s^2 + b_1s + b_0} \left[\frac{m}{N}\right] \tag{11}$$

where the coefficients a_n and b_n are listed in the Table 1.

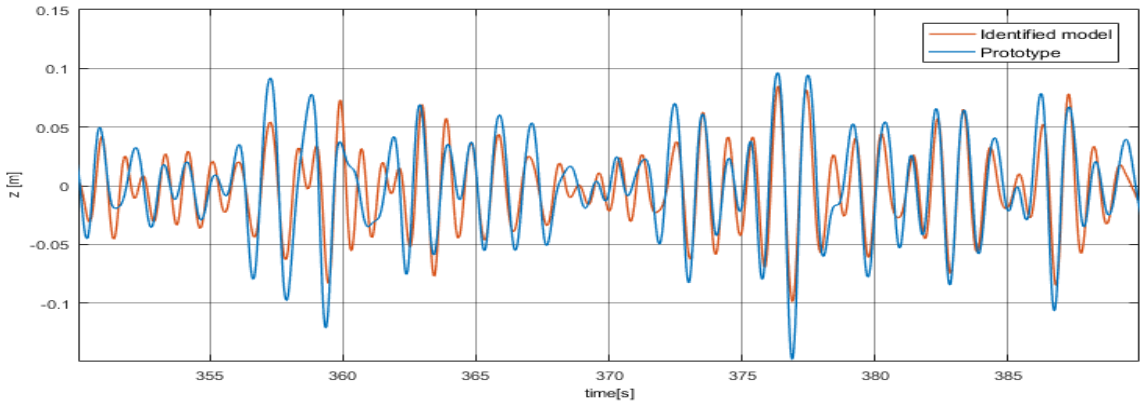

Figure 2. Buoy position: model identified for WEC prototype vs real response of the prototype.

Table 1. Model coefficients identified for the WEC system.

Coefficient	Value	Coefficient	Value	Coefficient	Value	Coefficient	Value
—	—	b_9	88.49	—	—	—	—
a_8	2.443e-06	b_8	1.462e05	a_{K_8}	1.218e03	—	—
a_7	2.162e-04	b_7	6.681e06	a_{K_7}	2.297e05	b_{K_7}	88.492
a_6	3.570e-01	b_6	4.476e09	a_{K_6}	1.889e08	b_{K_6}	1.462e05
a_5	16.32	b_5	1.341e10	a_{K_5}	2.595e10	b_{K_5}	6.68e06
a_4	1.093e04	b_4	6.359e10	a_{K_4}	6.268e12	b_{K_4}	4.476e09
a_3	3.268e04	b_3	8.594e10	a_{K_3}	5.617e14	b_{K_3}	1.338e10
a_2	1.304e05	b_2	1.824e11	a_{K_2}	1.684e15	b_{K_2}	5.337e10
a_1	1.353e05	b_1	1.129e11	a_{K_1}	4.684e15	b_{K_1}	5.537e10
a_0	1.599e05	b_0	1.294e11	a_{K_0}	1.407e15	b_{K_0}	6.545e10

In order to validate the identification methodology proposed in this paper, the identification process for the prototype of Figure 3 is carried out. Then, the response of the identified prototype model is compared with the real response registered in [27]. For this purpose, to the identified model the temporal series of forces recorded (see Figure 2) are applied.

Figure 3. WEC prototype of the W2POWER platform, [27].

2.3. Treatment of the mathematical model for the design of MPCs

In order to ensure safe behaviour and reduce mechanical fatigue in PWAs systems, a model that allows to be imposed constraints on the oscillation speed and position of the buoy is necessary. For this reason, a brief study of the identified model (11) is needed. By representing in the state space, it can be verified that the system obtained is not completely controllable, and therefore, it is not a minimal realization [32]. Furthermore, it is not enough to reduce the model (11) to its minimum order, since, except for the system output (z), the other state variables lack physical sense and this does not allow to impose directly speed constraints (w). As a solution, we study the transfer function (9) that defines the dynamics of the radiation force. Representing (9) in the state space, it can be seen how the model obtained is not of minimum order. Therefore, the system is minimized by obtaining (12). Note that the state variables of this model (x_r) will not be controlled, so it is not necessary that they have physical sense.

$$\begin{aligned} \dot{x}_r(t) &= A_r x_r(t) + B_r w(t) \\ Fr_{K_r}(t) &= C_r x_r(t) + D_r w(t) \end{aligned} \tag{12}$$

where the matrix A_r, B_r, C_r y D_r are given by (13).

Preprints (www.preprints.org) | NOT PEER-REVIEWED | Posted: 28 September 2018 doi:10.20944/preprints201809.0556.v1

Peer-reviewed version available at Energies 2018, 11, 2857; doi:10.3390/en11102857

$$A_r = \begin{pmatrix} -3.0044 & -1.4736 & -0.3820 & -0.2258 \\ 8.1656 & 0.0180 & 0.0041 & 0.0025 \\ 0.0015 & 4.0015 & 0.0004 & 0.0002 \\ -0.0000 & -0.0000 & 2.0000 & -0.0000 \end{pmatrix}, \quad B_r = \begin{pmatrix} 121.3816 \\ -1.3375 \\ -0.1201 \\ 0.0005 \end{pmatrix}$$
$$C_r = 10^3 \begin{pmatrix} 1.0083 & 0.3683 & 0.2624 & 0.0377 \end{pmatrix}, \qquad D_r = 1218.70 \tag{13}$$

A realistic model must consider the dynamics of the power take-off system. Given the similarity between the Wavestar system and the WEC studied in this work, the PTO model proposed in [22] is used, where the dynamics of the PTO is modeled according to (8). By representing this model in the state space, with the parameters indicated in [22], we obtain the matrix (14), where observable canonical form has been chosen. Thus, one of the state variables corresponds to the output of the PTO, so it is possible for MPC controllers to impose restrictions on the output of the actuator.

$$A_{pto} = \begin{pmatrix} -8.7965 & 1.0000 \\ -157.9137 & 0 \end{pmatrix}, \quad B_{pto} = \begin{pmatrix} 0 \\ 157.9137 \end{pmatrix}, \quad C_{pto} = \begin{pmatrix} 1 & 0 \end{pmatrix}, \quad D_{pto} = 0 \tag{14}$$

After that, in this paper we propose (15) as one of the design models. On this model an MPC controller can impose restrictions on the following state variables: force applied by the PTO (x_{pto_1}), speed (w) and buoy position (z). This model is similar to the one proposed in [8,12], but also considering the dynamics of the PTO system.

$$\underbrace{\begin{pmatrix} \dot{z} \\ \dot{w} \\ \dot{x}_r \\ \dot{x}_{pto} \end{pmatrix}}_{\dot{x}} = \underbrace{\begin{pmatrix} 0 & 1 & 0 & 0 \\ -\frac{k_{res}}{m_T} & -\frac{1}{m_T}D_r & -\frac{1}{m_T}C_r & \frac{1}{m_T}C_{pto} \\ 0 & B_r & A_r & 0 \\ 0 & 0 & 0 & A_{pto} \end{pmatrix}}_{A_{WEC}} \underbrace{\begin{pmatrix} z \\ w \\ x_r \\ x_{pto} \end{pmatrix}}_{x} + \underbrace{\begin{pmatrix} 0 \\ 0 \\ 0 \\ B_{pto} \end{pmatrix}}_{B_{WEC_u}} F_u + \underbrace{\begin{pmatrix} 0 \\ \frac{1}{m_T} \\ 0 \\ 0 \end{pmatrix}}_{B_{WEC_{F_e}}} F_e$$
$$\underbrace{\begin{pmatrix} z \\ w \end{pmatrix}}_{y} = \underbrace{\begin{pmatrix} 1 & 0 & 0 & 0 \\ 0 & 1 & 0 & 0 \end{pmatrix}}_{C_{WEC}} \underbrace{\begin{pmatrix} z \\ w \\ x_r \\ x_{pto} \end{pmatrix}}_{x} \tag{15}$$

where $m_T = m + m_\infty$, the matrices I (unit matrix) and 0 have the required size according to their location and the parameters not yet presented are listed in the Table 2.

Table 2. Parameters of the models (15) and (16) for the WEC system.

Symbol	Description	Value
k_{res}	Hydrostatic restoring coefficient	809325 N/m
B_{aprox}	Stationary approximation to system damping	21497 Ns/m
m	Mass of water displaced by the buoy at rest	241601.9 kg
m_∞	Mass of water added	167700 kg

Preprints (www.preprints.org) | NOT PEER-REVIEWED | Posted: 28 September 2018 doi:10.20944/preprints201809.0556.v1

Peer-reviewed version available at Energies 2018, 11, 2857; doi:10.3390/en11102857

2.3.1. Simplified model for the design

For the design of some MPCs we use a simplified model (16). It differs from the previous model (15) in that it does not consider the dynamics of the radiation force or the PTO system. Modeling used in [9–11,13,14]. The Figure 4 shows a comparison of the outputs of the simplified model and the complete model.

$$\underbrace{\begin{pmatrix}\dot{z}\\ \dot{w}\end{pmatrix}}_{\dot{x}} = \underbrace{\begin{pmatrix}0 & 1\\ -\frac{k_{res}}{m_T} & -\frac{B_{aprox}}{m_T}\end{pmatrix}}_{A_{WECr}} \underbrace{\begin{pmatrix}z\\ w\end{pmatrix}}_{x} + \underbrace{\begin{pmatrix}0\\ \frac{1}{m_T}\end{pmatrix}}_{B_{WECr}} (F_u + F_e)$$
$$\underbrace{\begin{pmatrix}z\\ w\end{pmatrix}}_{y} = \underbrace{\begin{pmatrix}1 & 0\\ 0 & 1\end{pmatrix}}_{C_{WECr}} \underbrace{\begin{pmatrix}z\\ w\end{pmatrix}}_{x} \tag{16}$$

where $m_T = m + m_\infty$ and the parameters are listed in the Table 2.

3. Model Predictive Control for Point Absorber Wave

This section details the design of the commonly used MPC controllers for PWAs. Moreover, in this work two MPCs are proposed based on the addition of an embedded integrator. In order to make a complete design, all the MPCs designed take into account constraints and the possibility of relaxing them in the case of non-feasibility in the cost function. In particular, these constraints are applied to the control force of the PTO system, the position of the buoy and its oscillation speed. However, in case of non-feasibility, only soft-constrains are applied to the position and speed of the system. Because the PTO is an actuator whose physical limit cannot be exceeded. Finally, for each controller a sampling period of Tm is set, which is used to discretize the mathematical model employing the transformed z zero-order-hold.

3.1. MPC_1

The cost function that minimizes this controller directly considers the maximization of extracted power. As a design model it uses (16), for which the state vector estimated for a prediction horizon M and a control horizon N is defined according to Equation (17), [18,19].

$$X = \underbrace{\begin{bmatrix}A\\ A^2\\ A^3\\ \vdots\\ A^M\end{bmatrix}}_{Jx_{(Mn\times n)}} x_k + \underbrace{\begin{bmatrix}B & 0 & 0 & \dots & 0\\ AB & B & 0 & \dots & 0\\ A^2B & AB & B & \dots & 0\\ \vdots & \vdots & \vdots & \ddots & \vdots\\ A^{M-1}B & A^{M-2}B & A^{M-3}B & \dots & A^{M-N}B\end{bmatrix}}_{Ju_{(Mn\times N)}} (F_{pto} + F_e) \tag{17}$$

where X represents the estimated state vector for a prediction horizon M, x_k represents the state vector at the current instant, the matrices A and B are obtained from the model (16) discretized, n is the order of the model and, F_{pto} and F_e are vectors that contain the force applied by the PTO and the excitation force for whole control horizon N, respectively.

In a more reduced form, the above equation can be expressed as:

$$X = J_x x_k + J_u(F_{pto} + F_e) \tag{18}$$

Preprints (www.preprints.org) | NOT PEER-REVIEWED | Posted: 28 September 2018 doi:10.20944/preprints201809.0556.v1

Peer-reviewed version available at Energies 2018, 11, 2857; doi:10.3390/en11102857

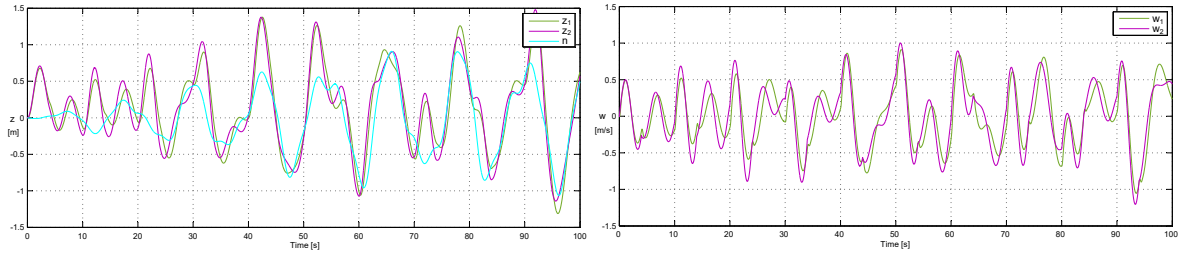

Figure 4. Comparison of models: complete ($z1$, $w1$) vs simplified ($z2$, $w2$). The height of the wave is n.

On the other side, the mechanical power generated is given by (19) [10,12,24]. Expressing the power generated for the entire prediction horizon is obtained (20).

$$P_{gen}(t) = -F_{pto}(t)w(t) \tag{19}$$

$$P_{gen} = -W^T F_{pto} \tag{20}$$

where W and F_{pto} are vectors with length M, which represent the speed and control force for the entire prediction horizon, respectively.

By replacing (18) in (20),

$$\begin{aligned} P_{gen} &= -(S_w X)^T F_{pto} \\ P_{gen} &= -(S_w(J_x x_k + J_u F_{pto} + J_u F_e))^T F_{pto} \end{aligned} \tag{21}$$

where S_w is a selector matrix for speed w (size $M \times Mn$).

Developing (21) and grouping in terms of least squares is obtained the cost function:

$$J(F_{pto}) = \frac{1}{2} {F_{pto}}^T \underbrace{({J_u}^T {S_w}^T + R)}_{H} F_{pto} + \frac{1}{2} \underbrace{({F_e}^T {J_u}^T {S_w}^T + {x_k}^T {J_x}^T {S_w}^T)}_{b} F_{pto} \tag{22}$$

where the matrix R weights the control effort.

In addition, constraints are imposed to: force demanded to the PTO, position and speed of the buoy (24). Therefore, the cost function (22) with constraints is defined as:

$$\begin{aligned} J(F_{pto}) =& \frac{1}{2} {F_{pto}}^T H F_{pto} + \frac{1}{2} b F_{pto} \\ A_g F_{pto} \leq& B_g \end{aligned} \tag{23}$$

where $A_g = [A_1 \quad A_2 \quad A_3]^T$ y $B_g = [B_1 \quad B_2 \quad B_3]^T$, see Equation (24).

$$\begin{gathered} \underbrace{\begin{bmatrix} I \\ -I \end{bmatrix}}_{A_1} F_{pto} \leq \underbrace{\begin{bmatrix} F_{PTO_{max}} \\ -F_{PTO_{min}} \end{bmatrix}}_{B_1}, \quad \underbrace{\begin{bmatrix} S_z J_u \\ -S_z J_u \end{bmatrix}}_{A_2} F_{pto} \leq \underbrace{\begin{bmatrix} Z_{n_{max}} - S_z(J_x x_k + J_u F_e) \\ -Z_{n_{min}} + S_z(J_x x_k + J_u F_e) \end{bmatrix}}_{B_2} \\ \underbrace{\begin{bmatrix} S_w J_u \\ -S_w J_u \end{bmatrix}}_{A_3} F_{pto} \leq \underbrace{\begin{bmatrix} W_{n_{max}} - S_w(J_x x_k + J_u F_e) \\ -W_{n_{min}} + S_w(J_x x_k + J_u F_e) \end{bmatrix}}_{B_3} \end{gathered} \tag{24}$$

where S_z is a selector matrix for position (size $M \times Mn$), the vectors $F_{PTO_{max}}$ and $F_{PTO_{min}}$ (size $N \times 1$) define the nominal limits of the force applied by the PTO, the vectors $W_{n_{max}}$, $W_{n_{min}}$, $Z_{n_{max}}$ and $Z_{n_{min}}$ (size $M \times 1$) define the nominal limits of the buoy position and oscillation speed, respectively. In addition, the matrices I (unit matrix) and 0 have the required size according to their location.

Preprints (www.preprints.org) | NOT PEER-REVIEWED | Posted: 28 September 2018 doi:10.20944/preprints201809.0556.v1

Peer-reviewed version available at Energies 2018, 11, 2857; doi:10.3390/en11102857

In the case of non-feasibility are applied soft constraints to the position and speed of the system. So, the cost function (22) would be defined as:

$$J(F_{pto}, \varepsilon_z, \varepsilon_w) = \frac{1}{2} {F_{pto}}^T H F_{pto} + b F_{pto} + {\varepsilon_z}^T W_{\varepsilon_z} \varepsilon_z + {\varepsilon_w}^T W_{\varepsilon_w} \varepsilon_w \tag{25}$$

where ε_z and ε_w represent the relaxation applied to position and speed along the prediction horizon M and the matrices $W_{varepsilon_z}$ and $W_{varepsilon_w}$ (size $M \times M$) weight these slacks.

By regrouping terms and adding soft restrictions (27), the cost function (25) can be expressed as:

$$\begin{aligned} J(\beta) =& \frac{1}{2} \beta^T \begin{bmatrix} H & 0 & 0 \\ 0 & W_{\varepsilon_z} & 0 \\ 0 & 0 & W_{\varepsilon_w} \end{bmatrix} \beta + \begin{bmatrix} b & 0 & 0 \end{bmatrix} \beta \\ & A_g \beta \leq B_g \end{aligned} \tag{26}$$

where $\beta = [F_{pto} \quad \varepsilon_z \quad \varepsilon_w]^T$, with size $(N + 2M) \times 1$, $A_g = [A_1 \quad A_2 \quad A_3 \quad A_4 \quad A_5]^T$ and $B_g = [B_1 \quad B_2 \quad B_3 \quad B_4 \quad B_5]^T$, see Equation (27). Matrices 0 have the required size according to their location.

$$\begin{gathered} \underbrace{\begin{bmatrix} S_z J_u & -I & 0 \\ -S_z J_u & -I & 0 \end{bmatrix}}_{A_2} \beta \leq \underbrace{\begin{bmatrix} Z_{n_{max}} - S_z(J_x x_k + J_u F_e) \\ -Z_{n_{min}} + S_z(J_x x_k + J_u F_e) \end{bmatrix}}_{B_2}, \quad \underbrace{\begin{bmatrix} S_w J_u & 0 & I \\ -S_w J_u & 0 & I \end{bmatrix}}_{A_3} \beta \leq \underbrace{\begin{bmatrix} W_{n_{max}} - S_w(J_x x_k + J_u F_e) \\ -W_{n_{min}} + S_w(J_x x_k + J_u F_e) \end{bmatrix}}_{B_3} \\ \underbrace{\begin{bmatrix} I & 0 & 0 \\ -I & 0 & 0 \end{bmatrix}}_{A_1} \beta \leq \underbrace{\begin{bmatrix} F_{PTO_{max}} \\ -F_{PTO_{min}} \end{bmatrix}}_{B_1}, \quad \underbrace{\begin{bmatrix} 0 & I & 0 \\ 0 & -I & 0 \end{bmatrix}}_{A_4} \beta \leq \underbrace{\begin{bmatrix} \kappa_z \\ 0 \end{bmatrix}}_{B_4}, \quad \underbrace{\begin{bmatrix} 0 & 0 & I \\ 0 & 0 & -I \end{bmatrix}}_{A_5} \beta \leq \underbrace{\begin{bmatrix} \kappa_w \\ 0 \end{bmatrix}}_{B_5} \end{gathered} \tag{27}$$

where κ_z and κ_w are vectors (size $M \times 1$) that represent the maximum slack allowed for position and speed, respectively. The matrices I (unit matrix) and 0 have the required size according to their location.

3.2. MPC_2

This controller uses the simplified model (16). Its cost function is based on maximizing the extracted power by tracking a setpoint for the system speed (w_{ref}) along a prediction horizon M,

$$J = (\tilde{w} - w_{ref})^T Q (\tilde{w} - w_{ref}) + {F_{pto}}^T R F_{pto} \tag{28}$$

where Q and R are diagonal matrices of size $(M \times M)$ and $(N \times N)$ that weight the tracking error and the control effort, respectively.

Substituting (18) in (28), the cost function for this controller can be written as (29).

$$J(F_{pto}) = (\underbrace{J_x x_k + J_u F_{pto} + J_u F_e}_{f} - w_{ref})^T Q (\underbrace{J_x x_k + J_u F_{pto} + J_u F_e}_{f} - w_{ref}) + {F_{pto}}^T R F_{pto} \tag{29}$$

By developing the cost function (29) and grouping terms the following expression is obtained:

$${F_{pto}}^T \underbrace{(J_u^T \delta J_u + R)}_{H} F_{pto} + 2 \underbrace{(f - w_{ref})^T Q J_u}_{b} F_{pto} + \underbrace{(f - w_{ref})^T Q (f - w_{ref})}_{l} \tag{30}$$

Note that the term l can be ignored when the cost function is minimized, because it does not depend on the variable to be optimized (F_{pto}), remaining:

$$J(F_{pto}) = \frac{1}{2}{F_{pto}}^T \underbrace{(J_u^T \delta J_u + R)}_{H} F_{pto} + \underbrace{(J_x x_k + J_u F_{pto} + J_u F_e - w_{ref})^T Q J_u}_{b} F_{pto} \tag{31}$$

The constraints imposed on this cost function can be expressed in the same way as in the MPC_1 controller. Using (23) for hard constraints and (26) for soft constraints. On the other hand, the reference trajectory or setpoint for the speed is defined by the approach proposed in [29], $w_{ref} = F_e/2B_{aprox}$.

3.3. MPC_3

This is a contribution made in this work. This controller uses the simplified model (16) to which an embedded integrator has been added according to the theory of predictive controllers in the state space [18,19]. Its cost function is based on the maximization of the extracted power through the tracking of a setpoint for the system speed. To add the integrator it is necessary to multiply the model (16) discretized by the operator $\triangle = 1 - z^{-1}$. Regrouping terms, an extended state vector is defined as:

$$\begin{gathered} \underbrace{\begin{bmatrix} \triangle x(t+1) \\ y(t+1) \end{bmatrix}}_{x_e(t+1)} = \underbrace{\begin{bmatrix} A & 0 \\ CA & I \end{bmatrix}}_{A_e} \underbrace{\begin{bmatrix} \triangle x(t) \\ y(t) \end{bmatrix}}_{x_e(t)} + \underbrace{\begin{bmatrix} B \\ CB \end{bmatrix}}_{B_e} (\triangle F_{pto}(t) + \triangle F_e(t)) \\ y(t) = \underbrace{\begin{bmatrix} 0 & I \end{bmatrix}}_{C_e} \underbrace{\begin{bmatrix} \triangle x(t) \\ y(t) \end{bmatrix}}_{x_e(t)} \end{gathered} \tag{32}$$

where the output vector $y(t)$ is formed by the position and speed of the WEC system, $\triangle x(t)$ represents the state vector increment, the matrices A, B and C are from the model (16) discretized and the matrices 0 have the required size according to their location.

Using the extended model (32), the prediction of the outputs (z, w) is defined for a prediction horizon M and a control horizon N according:

$$Y = \underbrace{\begin{bmatrix} CA \\ CA^2 \\ CA^3 \\ \vdots \\ CA^M \end{bmatrix}}_{F_{(2M \times n_e)}} X_e + \underbrace{\begin{bmatrix} CB & 0 & 0 & \dots & 0 \\ CAB & CB & 0 & \dots & 0 \\ CA^2B & CAB & CB & \dots & 0 \\ \vdots & \vdots & \vdots & \ddots & \vdots \\ CA^{M-1}B & CA^{M-2}B & CA^{M-3}B & \dots & CA^{M-N}B \end{bmatrix}}_{G_{(2M \times N)}} (\triangle F_{pto} + \triangle F_e) \tag{33}$$

where $n_e = n + j$ represents the order of the extended model and j its number of outputs. In the matrices A B and C the sub-index e has been omitted to get a clearer notation.

By adding the embedded integrator, this controller minimizes a cost function that gets the optimal increase in control force (F_{pto}) for the full control horizon N,

$$J = (\tilde{w} - w_{ref})^T Q (\tilde{w} - w_{ref}) + \triangle {F_{pto}}^T R \triangle F_{pto} \tag{34}$$

where Q and R are diagonal matrices of size $(M \times M)$ and $(N \times N)$ that weighs the tracking error and the control effort, respectively.

Replacing the output prediction (33) in (34) and obviating the independent term of $\triangle F_{pto}$:

Preprints (www.preprints.org) | NOT PEER-REVIEWED | Posted: 28 September 2018 doi:10.20944/preprints201809.0556.v1

Peer-reviewed version available at Energies 2018, 11, 2857; doi:10.3390/en11102857

$$J(\triangle F_{pto}) = \frac{1}{2}\triangle {F_{pto}}^T \underbrace{(G^T \delta G + R)}_{H} \triangle F_{pto} + \underbrace{(Fx_{e_k} + G\triangle F_e - w_{ref})^T QG}_{b} \triangle F_{pto} \tag{35}$$

In addition, constraints are added to the demanded force on the PTO, position and speed of the system (37). Therefore, the cost function (35) subject to the restrictions is defined as:

$$\begin{aligned} J(\triangle F_{pto}) =& \frac{1}{2}\triangle {F_{pto}}^T H \triangle F_{pto} + b\triangle F_{pto} \\ A_g \triangle F_{pto} \leq& B_g \end{aligned} \tag{36}$$

where $A_g = [A_1 \quad A_2 \quad A_3]^T$ y $B_g = [B_1 \quad B_2 \quad B_3]^T$, see Equation (37).

$$\begin{gathered} \underbrace{\begin{bmatrix} T \\ -T \end{bmatrix}}_{A_1} \triangle F_{pto} \leq \underbrace{\begin{bmatrix} F_{PTO_{max}} \\ -F_{PTO_{min}} \end{bmatrix}}_{B_1}, \quad \underbrace{\begin{bmatrix} S_z G \\ -S_z G \end{bmatrix}}_{A_2} \triangle F_{pto} \leq \underbrace{\begin{bmatrix} Z_{n_{max}} - S_z(Fx_{e_k} + G\triangle F_e) \\ -Z_{n_{min}} + S_z(Fx_{e_k} + G\triangle F_e) \end{bmatrix}}_{B_2} \\ \underbrace{\begin{bmatrix} S_w G \\ -S_w G \end{bmatrix}}_{A_3} \triangle F_{pto} \leq \underbrace{\begin{bmatrix} W_{n_{max}} - S_w(Fx_{e_k} + G\triangle F_e) \\ -W_{n_{min}} + S_w(Fx_{e_k} + G\triangle F_e) \end{bmatrix}}_{B_3} \end{gathered} \tag{37}$$

where S_z and S_w are selectors matrices for z and w (size $M \times Mn$), T is a lower triangular matrix (size $M \times N$), the vectors $F_{PTO_{max}}$ and $F_{PTO_{min}}$ (size $N \times 1$) define the nominal limits of the force applied by the PTO, the vectors $W_{n_{max}}$, $W_{n_{min}}$, $Z_{n_{max}}$ and $Z_{n_{min}}$ (size $M \times 1$) define the nominal limits of the buoy position and oscillation speed, respectively. In addition, the matrices I (unit matrix) and 0 have the required size according to their location.

Furthermore, if the cost function is not feasible (36), sotf constraints are applied,

$$\begin{aligned} J(\beta) =& \frac{1}{2}\beta^T \begin{bmatrix} H & 0 & 0 \\ 0 & W_{\varepsilon_z} & 0 \\ 0 & 0 & W_{\varepsilon_w} \end{bmatrix} \beta + \begin{bmatrix} b & 0 & 0 \end{bmatrix} \beta \\ A_g \beta \leq& B_g \end{aligned} \tag{38}$$

where $A_g = [A_1 \quad A_2 \quad A_3 \quad A_4 \quad A_5]^T$ y $B_g = [B_1 \quad B_2 \quad B_3 \quad B_4 \quad B_5]^T$, see Equation (38).

$$\begin{gathered} \underbrace{\begin{bmatrix} T & 0 & 0 \\ -T & 0 & 0 \end{bmatrix}}_{A_1} \beta \leq \underbrace{\begin{bmatrix} F_{PTO_{max}} \\ -F_{PTO_{min}} \end{bmatrix}}_{B_1} \\ \underbrace{\begin{bmatrix} S_z G & -I & 0 \\ -S_z G & -I & 0 \end{bmatrix}}_{A_2} \beta \leq \underbrace{\begin{bmatrix} Z_{n_{max}} - S_z(Fx_{e_k} + G\triangle F_e) \\ -Z_{n_{min}} + S_z(Fx_{e_k} + G\triangle F_e) \end{bmatrix}}_{B_2}, \quad \underbrace{\begin{bmatrix} 0 & I & 0 \\ 0 & -I & 0 \end{bmatrix}}_{A_4} \beta \leq \underbrace{\begin{bmatrix} \kappa_z \\ 0 \end{bmatrix}}_{B_4} \\ \underbrace{\begin{bmatrix} S_w G & 0 & I \\ -S_w G & 0 & I \end{bmatrix}}_{A_3} \beta \leq \underbrace{\begin{bmatrix} W_{n_{max}} - S_w(Fx_{e_k} + G\triangle F_e) \\ -W_{n_{min}} + S_w(Fx_{e_k} + G\triangle F_e) \end{bmatrix}}_{B_3}, \quad \underbrace{\begin{bmatrix} 0 & 0 & I \\ 0 & 0 & -I \end{bmatrix}}_{A_5} \beta \leq \underbrace{\begin{bmatrix} \kappa_w \\ 0 \end{bmatrix}}_{B_5} \end{gathered} \tag{39}$$

where κ_z and κ_w are vectors (size $M \times 1$) that represent the maximum slack allowed for z and w, respectively. The matrices I (unit matrix) and 0 have the required size according to their location.

3.4. MPC_4

This controller is made using the model (15). The cost function that minimizes this controller is directly focused on the maximization of extracted power. The matrix development needed to express this controller as a least squares problem is analogous to that presented for controller MPC_1. Although, when considering the dynamics of the PTO system the Equation (18) should be redefined as:

$$X = J_x x_k + J_u F_{pto} + J_f F_e \tag{40}$$

where J_x is a matrix already defined in the equation (17), while the matrices J_u and J_f are given by:

$$J_u = \begin{bmatrix} B_u & 0 & 0 & \dots & 0 \\ AB_u & B_u & 0 & \dots & 0 \\ A^2B_u & AB_u & B_u & \dots & 0 \\ \vdots & \vdots & \vdots & \ddots & \vdots \\ A^{M-1}B_u & A^{M-2}B_u & A^{M-3}B_u & \dots & A^{M-N}B_u \end{bmatrix}$$

$$J_f = \begin{bmatrix} B_{F_e} & 0 & 0 & \dots & 0 \\ AB_{F_e} & B_{F_e} & 0 & \dots & 0 \\ A^2B_{F_e} & AB_{F_e} & B_{F_e} & \dots & 0 \\ \vdots & \vdots & \vdots & \ddots & \vdots \\ A^{M-1}B_{F_e} & A^{M-2}B_{F_e} & A^{M-3}B_{F_e} & \dots & A^{M-N}B_{F_e} \end{bmatrix} \tag{41}$$

where A, B_u and B_{F_e} are obtained by discretizing A_{WEC}, B_{WEC_u} and $B_{WEC_{F_e}}$ of the model (15).

The cost function to be minimized by this controller can be expressed according to (42). Its development is analogous to that carried out for the controller MPC_1.

$$J(F_{pto}) = \frac{1}{2} {F_{pto}}^T \underbrace{\left({J_u}^T {S_w}^T + R\right)}_{H} F_{pto} + \frac{1}{2} \underbrace{\left({F_e}^T {J_f}^T {S_w}^T + {x_k}^T {J_x}^T {S_w}^T\right)}_{b} F_{pto} \tag{42}$$

In addition, the nominal constraints imposed on the system must be added, which are defined in the same way as in the controller MPC_1, Equation (24). Although in this case, it must be considered that the state vector prediction is given by Equation (40). Therefore, the cost function (42) subject to the constraints is defined as:

$$\begin{aligned} J(F_{pto}) =& \frac{1}{2} {F_{pto}}^T H F_{pto} + \frac{1}{2} b F_{pto} \\ A_g F_{pto} \leq& B_g \end{aligned} \tag{43}$$

where $A_g = [A_1 \quad A_2 \quad A_3]^T$ y $B_g = [B_1 \quad B_2 \quad B_3]^T$, see Equation (24).

Finally, in the case of non-feasibility in the function (48) soft constraints will be applied to the system. These can be expressed in a similar way to the development shown for the MPC_1 Equation (27). Although, in this case it must be considered that the prediction of the state vector is given by the equation (40). Therefore, the cost function of this controller subject to soft constraints is given by:

$$\begin{aligned} J(\beta) =& \frac{1}{2} \beta^T \begin{bmatrix} H & 0 & 0 \\ 0 & W_{\varepsilon_z} & 0 \\ 0 & 0 & W_{\varepsilon_w} \end{bmatrix} \beta + \begin{bmatrix} b & 0 & 0 \end{bmatrix} \beta \\ A_g \beta \leq& B_g \end{aligned} \tag{44}$$

where $A_g = [A_1 \quad A_2 \quad A_3 \quad A_4 \quad A_5]^T$ y $B_g = [B_1 \quad B_2 \quad B_3 \quad B_4 \quad B_5]^T$, see Equation (27).

Preprints (www.preprints.org) | NOT PEER-REVIEWED | Posted: 28 September 2018 doi:10.20944/preprints201809.0556.v1

Peer-reviewed version available at Energies 2018, 11, 2857; doi:10.3390/en11102857

3.5. MPC_5

This proposal is another contribution made in this work. This controller uses the model (15), which an embedded integrator has been added according to the theory of predictive controllers in the state space [18,19]. Its cost function to minimize is based on the maximization of the extracted power through the tracking of a setpoint for the speed of the system w_{ref}. As in the MPC_3, the state vector is extended by adding an embedded integrator (32). Although when considering the dynamics of the PTO system the prediction of the output vector for the full prediction horizon M is defined by:

$$Y = G_u \triangle F_{pto} + \underbrace{F x_{e_k} + G_f \triangle F_e}_{f} \tag{45}$$

where F is a matrix already defined in Equation (33) and the matrices G_u and G_f are given by:

$$G_u = \begin{bmatrix} C_e B_{e_u} & 0 & 0 & \dots & 0 \\ C_e A_e B_{e_u} & C_e B_{e_u} & 0 & \dots & 0 \\ C_e {A_e}^2 B_{e_u} & C_e A_e B_{e_u} & C_e B_{e_u} & \dots & 0 \\ \vdots & \vdots & \vdots & \ddots & \vdots \\ C_e {A_e}^{M-1} B_{e_u} & C_e {A_e}^{M-2} B_{e_u} & C_e {A_e}^{M-3} B_{e_u} & \dots & C_e {A_e}^{M-N} B_{e_u} \end{bmatrix}$$

$$G_f = \begin{bmatrix} C_e B_{e_{Fe}} & 0 & 0 & \dots & 0 \\ C_e A_e B_{e_{Fe}} & C_e B_{e_{Fe}} & 0 & \dots & 0 \\ C_e {A_e}^2 B_{e_{Fe}} & C_e A_e B_{e_{Fe}} & C_e B_{e_{Fe}} & \dots & 0 \\ \vdots & \vdots & \vdots & \ddots & \vdots \\ C_e {A_e}^{M-1} B_{e_{Fe}} & C_e {A_e}^{M-2} B_{e_{Fe}} & C_e {A_e}^{M-3} B_{e_{Fe}} & \dots & C_e {A_e}^{M-N} B_{e_{Fe}} \end{bmatrix} \tag{46}$$

where B_{e_u} and $B_{e_{Fe}}$ are obtained by discretizing the matrices that define the inputs of (15) extended.

Analogous to controller MPC_3, the cost function to be minimized can be expressed according to:

$$J(\triangle F_{pto}) = \frac{1}{2} \triangle {F_{pto}}^T \underbrace{({G_u}^T \delta G_u + R)}_{H} \triangle F_{pto} + \underbrace{(F x_{e_k} + G_f \triangle F_e - w_{ref})^T Q G_u}_{b} \triangle F_{pto} \tag{47}$$

In addition, it is necessary to add nominal constraints to the system (37), which are defined as in the controller MPC_3. However, in this case it must be considered that the prediction of the system outputs is given by (45). So, the cost function (47) subject to the constraint is defined as:

$$\begin{aligned} J(\triangle F_{pto}) =& \frac{1}{2} \triangle {F_{pto}}^T H \triangle F_{pto} + \frac{1}{2} b \triangle F_{pto} \\ & A_g \triangle F_{pto} \leq B_g \end{aligned} \tag{48}$$

where $A_g = [A_1 \quad A_2 \quad A_3]^T$ y $B_g = [B_1 \quad B_2 \quad B_3]^T$ see Equation (37).

Furthermore, in case of non-feasibility in the function (47), soft constraints are used. The soft-constrains are expressed analogous to the development made for controller MPC_3 Equation (39). Although, in this case the prediction of the system output is given by (45). Therefore, the cost function of this controller subject to soft constraints is defined as:

$$\begin{aligned} J(\beta) =& \frac{1}{2} \beta^T \begin{bmatrix} H & 0 & 0 \\ 0 & W_{\varepsilon_z} & 0 \\ 0 & 0 & W_{\varepsilon_w} \end{bmatrix} \beta + \begin{bmatrix} b & 0 & 0 \end{bmatrix} \beta \\ & A_g \beta \leq B_g \end{aligned} \tag{49}$$

donde $A_g = [A_1 \quad A_2 \quad A_3 \quad A_4 \quad A_5]^T$ y $B_g = [B_1 \quad B_2 \quad B_3 \quad B_4 \quad B_5]^T$, see Equation (39).

4. Study about performances and robustness

This section presents the results obtained from an in-depth study of the performance and robustness of the five MPCs designs. This study assumes that the system state vector and excitation force (F_e) for the whole prediction horizon (M) are known (note that this has the same effect in all MPCs). For this reason, the simulations are performed in an irregular sea state formed by the fifteen sinusoidal components listed in the Table 3. In addition, a comparison of the robustness of the designed MPCs is made, which focuses on the uncertainty added to the most significant identified parameters of the WEC system (m_{infty}, B_{aprox} and k_{res}). Note that when modifying the physical parameters of the WEC system the frequency response of the filter (10) is affected. Therefore, looking for a realistic comparative, it would be necessary to identify a new filter (6) for each added uncertainty. Given the high number of simulations required, applying different levels of uncertainty to each of the parameters, this is not feasible. For this reason, in this work the Morison model (7) is used to define F_e, allowing to modify more easily the excitation force caused by the wave in function of the added uncertainty.

Table 3. Sinusoidal components used for sea-state (values expressed in international units).

Component	Amplitude	Period	Phase	Component	Amplitude	Period	Phase
s_1	0.420	13.00	$-\pi$	s_9	0.200	9.00	0.00
s_2	0.520	12.50	1.5π	s_{10}	0.180	8.50	π
s_3	0.420	12.25	0.40	s_{11}	0.200	7.50	0.10
s_4	0.520	11.50	0.20	s_{12}	0.150	6.50	-0.77
s_5	0.450	11.25	0.11π	s_{13}	0.100	5.50	0.5π
s_6	0.300	10.50	-1.50	s_{14}	0.075	5.00	0.00
s_7	0.500	10.00	-0.33	s_{15}	0.020	3.70	0.12
s_8	0.210	9.50	0.78	—	—	—	—

Due to the WEC system of the W2POWER platform have not yet been built, so their operating limits and physical limits are not available. Therefore, these limits have been chosen on the basis of [12,15,16,22], whose WECs systems are similar to the system studied in this paper, see Table 4.

Table 4. Constraints for the WEC system.

Symbol	Description	Value
$F_{PTO_{max}}$	Maximum stationary force for power take-off system	450 KN
$F_{PTO_{min}}$	Minimum stationary force for power take-off system	-450 KN
$z_{n_{max}}$	Maximum nominal limit for buoy position	1.25 m
$z_{n_{min}}$	Minimum nominal limit for buoy position	-1.25 m
$w_{n_{max}}$	Maximum nominal limit for oscillation speed	1 m/s
$w_{n_{min}}$	Minimum nominal limit for oscillation speed	-1 m/s
$z_{f_{max}}$	Maximum physical limit for buoy position	1.7 m
$z_{f_{min}}$	Minimum physical limit for buoy position	-1.7 m
$w_{f_{max}}$	Maximum physical limit for oscillation speed	1.3 m/s
$w_{f_{min}}$	Minimum physical limit for oscillation speed	-1.3 m/s
κ_z	Maximum slack applied to the position nominal limit	0.45 m
κ_w	Maximum slack applied to the speed nominal limit	0.3 m/s

All simulations have been carried out using MatLab/Simulink. In particular, they use the Runge-Kutta integration method of order four (RK4) with an integration step of 1 ms and the function *quadprog* of MatLab [33] to solve the cost functions with constraints. Note that although the quadprog function provides F_u for the entire control horizon N, only the setpoint obtained for the current instant k is applied [18,19]. Furthermore, it is necessary to emphasize that the same effort has been spent in

Preprints (www.preprints.org) | NOT PEER-REVIEWED | Posted: 28 September 2018 doi:10.20944/preprints201809.0556.v1

Peer-reviewed version available at Energies 2018, 11, 2857; doi:10.3390/en11102857

the tuning of all controllers, looking for the maximum possible veracity in their comparison. As a result of this tuning, the parameters of the controllers are listed in the Table 5.

Table 5. Design parameters set for each MPC controller ($N = M$).

Controller	T_m $[s]$	M	R	Q	W_{ε_z}	W_{ε_w}
MPC_1	0.05	30	1.1×10^{-7}	—	1.0×10^{10}	1.0×10^{7}
MPC_2	0.04	30	1.0×10^{-7}	2.15×10^{4}	1.0×10^{7}	2.0×10^{9}
MPC_3	0.04	30	5.0×10^{-5}	1.475×10^{4}	5.0×10^{10}	1.0×10^{5}
MPC_4	0.05	30	4.5×10^{-7}	—	1.0×10^{8}	1.0×10^{4}
MPC_5	0.02	30	5.0×10^{-5}	1.75×10^{4}	1.0×10^{7}	1.0×10^{9}

Figures 5 and 6 show a comparison between the heights and oscillations speeds obtained by applying the five MPCs designs to the mathematical model (15). As can be seen, all controllers achieve to keep the WEC system within its physical operating limits, even though the wave scenario chosen is not favourable to the controllers. Because, as shown in Figure 7, the wave force becomes more than twice the stationary force that the PTO system can apply (recorded in the Table 4).

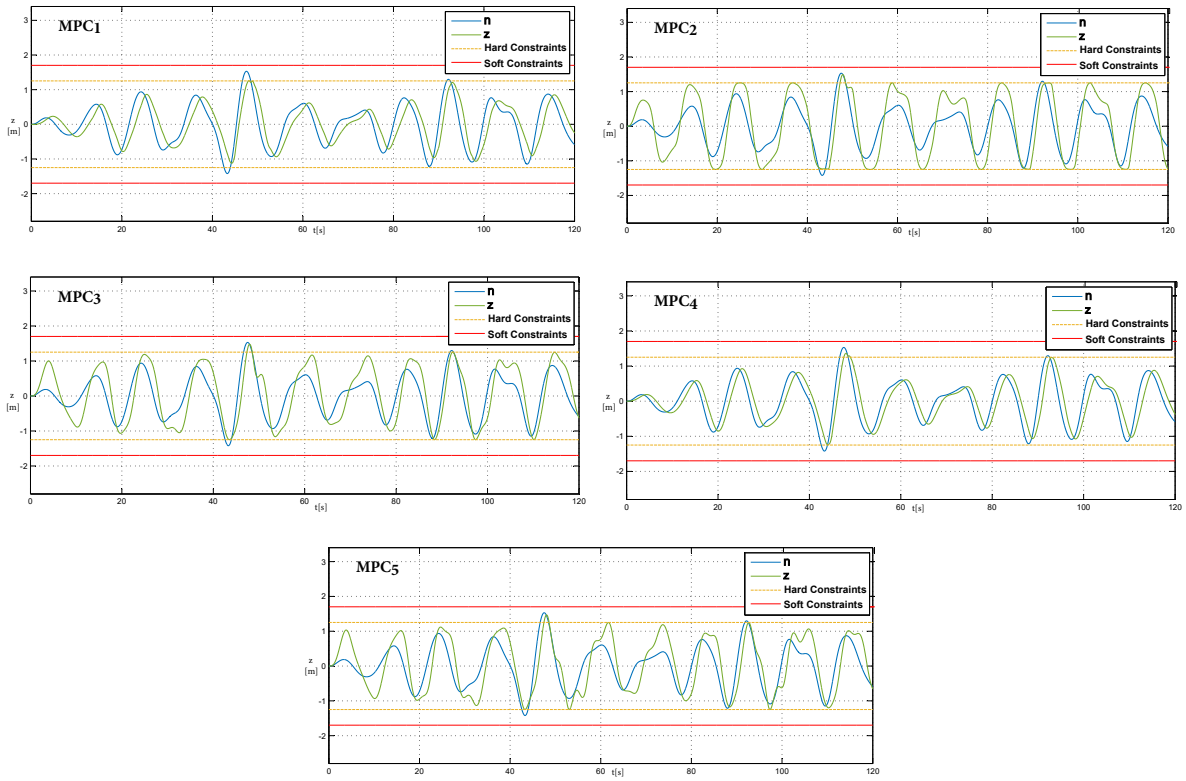

Figure 5. Comparison of the heights obtained in the WEC system when applying in simulation the five MPCs to the mathematical model (15).

On the other hand, the Figure 8 shows a comparative of the instantaneous mechanical powers generated by applying the MPCs designed in this work. In this comparative, it can be seen how applying the MPC_2 controller to the system gives the most irregular power. While the power generated with the MPC_3 controller, designed from the same model and following the same optimization criteria, is more clean. This is due to the fact that the MPC_1 controller is continuously applying soft constraints, because it does not carry out a good control of the force that the PTO system exerts on the WEC along the time (see Figure 7). On the other hand, the figures 5 and 6 show how the addiction of embedded

integrator (controller MPC_3) considerably improves the behavior of the system with respect to that obtained by applying the controller MPC_2. Because, the MPC_3 only exceeds the nominal limits of the position and oscillation speed on one occasion. In addition, the MPC_3 controller generates a clearer control signal than the MPC_2 (see Figure 7) and, as a consequence, the underdamped response of the PTO system decreases greatly. With this said, it can be concluded that the addition of the embedded integrator to the design model improves the performance of the WEC device with respect to: quality of the instantaneous power generated and reduction of mechanical fatigue (due to exceeding nominal limits).

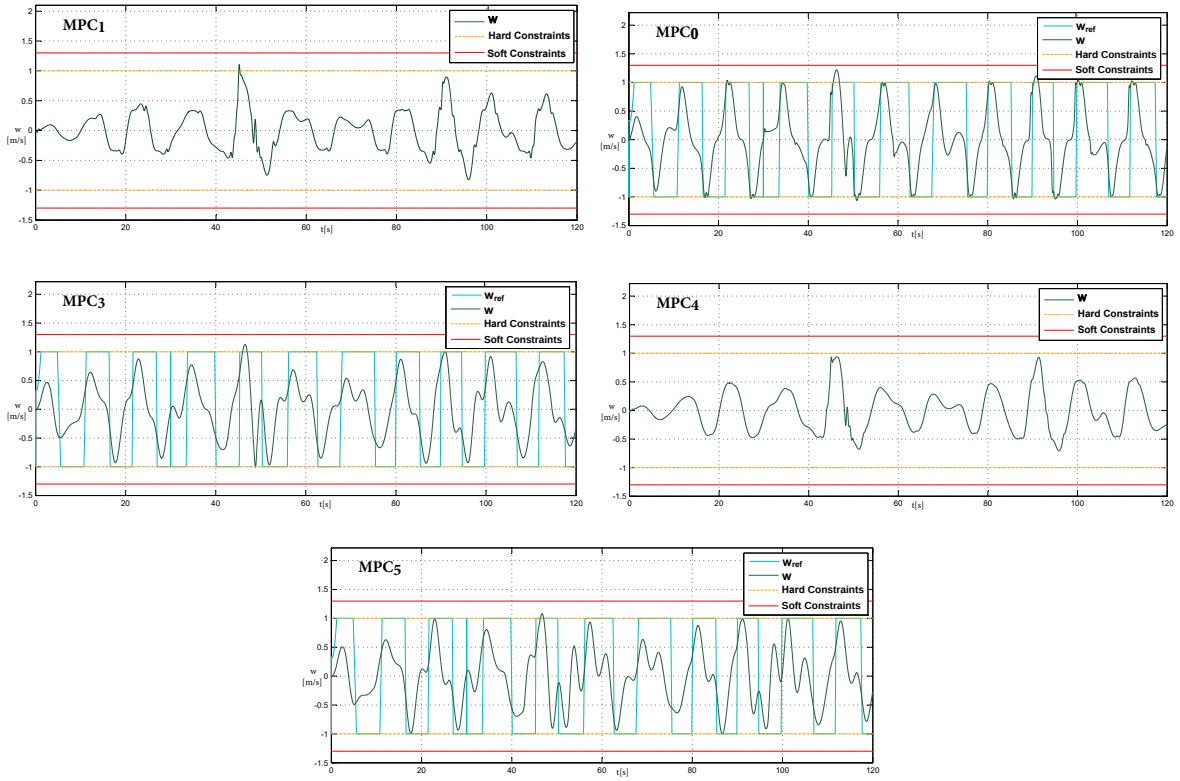

Figure 6. Comparison of the oscillation speed obtained in the WEC system when applying in simulation the five MPCs to the mathematical model (15).

With respect to the generated power, controllers that use the full model (15) as the design model get lower instantaneous power peaks than controllers that use the simplified model (16). This can be verified comparing the MPCs that follow the same optimization criteria but are based on different design models; the controller MPC_1 with MPC_4 and the controller MPC_3 with MPC_5. Specifically, the MPC_5 controller gets the best results, an average power of 97.04 kW which rarely has punctual peaks.

Table 6. Results obtained in the application of the five MPCs to the WEC system. The powers are expressed in kW. Note that $ONLP$ indicates Overshoot of Nominal Limits for Position and $ONLS$ indicates Overshoot of Nominal Limits for Speed.

Controller	$\bar{P}_{gen}$	$ONLH$	$ONLS$	$P_{gen_{Max}}$	$P_{gen_{Min}}$
MPC_1	88.94	0.0054	0.0023	785.5	-491.7
MPC_2	82.04	0.0259	0.0549	744.2	-369.4
MPC_3	97.58	0.0137	0.0100	507.3	-379.0
MPC_4	83.84	0.0156	0.0000	614.6	-237.3
MPC_5	97.04	0.0136	0.0070	482.7	-222.1

Preprints (www.preprints.org) | NOT PEER-REVIEWED | Posted: 28 September 2018 doi:10.20944/preprints201809.0556.v1

Peer-reviewed version available at Energies 2018, 11, 2857; doi:10.3390/en11102857

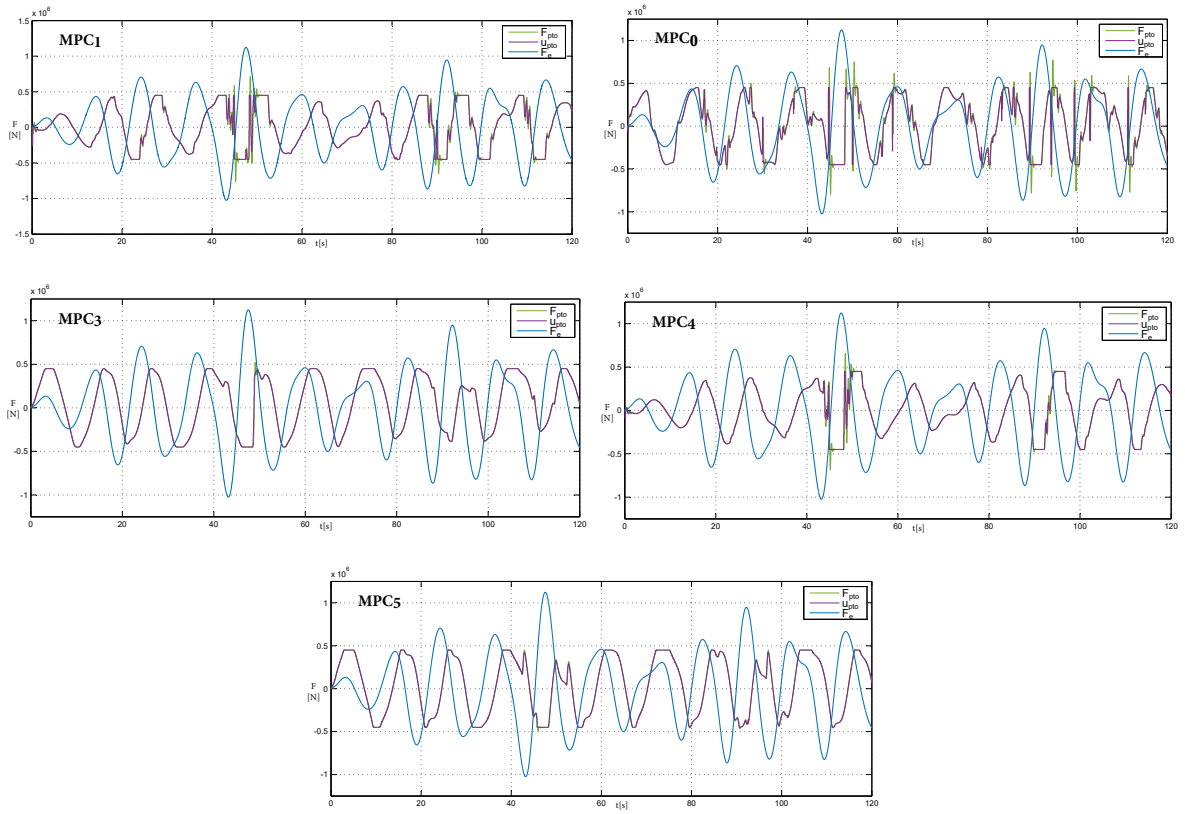

Figure 7. Comparisons between: wave force, force setpoint demanded to the PTO and real force produced by the PTO, by applying in simulation the five MPCs to the model (15).

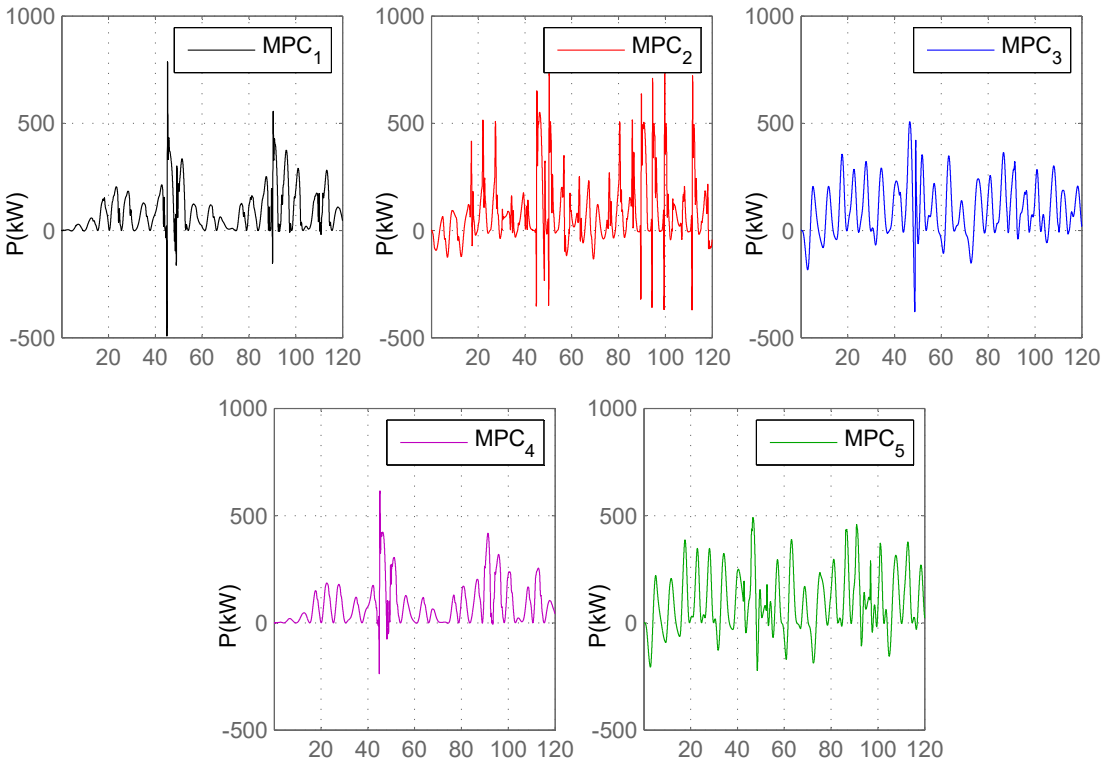

Figure 8. Instantaneous mechanical powers generated by applying in simulation the five MPCs to the mathematical model (15).

To support all that has been said previously, the Table 6 records the most significant quality indicators of the control performed by each MPC. First, this table shows the average mechanical powers generated by the WEC system when applying each controller. In this aspect, the MPC_3 controller achieves to generate more power, followed very closely by the MPC_5 and with a bit more distance by the MPC_1 controller. On the other side, the indicators $ONLP$ and $ONLS$ quantify the area of overshoot of the nominal limits of the position and oscillation speed, respectively. The controllers MPC_1 and MPC_4 are the ones that apply the least slack to the nominal limits, followed by the controller MPC_5. Therefore, with respect to the two optimization criteria compared in this paper, it can be concluded that the controllers that directly maximize the extracted power (MPC_1 and MPC_4) get less overshoot of the nominal limits. While the MPCs that use an optimization criterion based on the minimization of the error between the oscillation speed w and a setpoint w_{ref} for the whole prediction horizon (M) obtain a higher average power extraction. Finally, the last two columns of the Table 6 show the maximum and minimum power peaks obtained when applying each controller. In this aspect, the MPC_1 is the most unfavorable while the MPC_5 reports the best performance. Note that these power peaks will cause an oversizing of: electrical machines, power electronics, accumulators..

4.1. Robustness comparative

Another contribution of this work, and searching the greatest realism in the comparative of the designed controllers, uncertainty is added in the complete system model (15) to the most significant identified parameters (50). Added mass and dynamic of the radiation force, parameters that have been obtained through the openWEC software. On the other hand, the hydrostatic restoring coefficient K_{res}, a nonlinear parameter that has been linearized during the modeling of the WEC system.

$$\begin{aligned} F_{res}(t) &= -k_{res}(1+\triangle_{k_{res}})z(t) \\ \frac{Fr_{K_r}(s)}{W(s)} &= (1+\triangle_B)K_r(s) \\ Fr_{m_\infty}(t) &= m_\infty(1+\triangle_{m_\infty})\dot{w}(t) \end{aligned} \tag{50}$$

where $\triangle$ represents the added uncertainty in each parameters.

In addition, as mentioned above, by defining the excitation force with Morison's linear model facilitates the robustness analysis. Therefore, when modifying the physical parameters of the system, the external force that the wave causes on the system also varies. So, Equation (7) is redefined for this analysis as:

$$F_e(t) = m_\infty(1+\triangle_{m_\infty})\ddot{\eta}(t) + B(1+\triangle_B)\dot{\eta}(t) + k_{res}(1+\triangle_{k_{res}})\eta(t) \tag{51}$$

Note that for the same wave height, the excitation force can increase or decrease according to the uncertainty added in each parameter. Therefore, there will be situations where, for the sea state defined in the Table 3, the controller cannot keep the system within its physical limits. Since, the actuation force of the PTO system will be much lower than the excitation force. In this paper, this non-feasibility situation will be considered as the robustness limit that the controller can support. This limit is defined for the uncertainty added in each of the parameters (50). This non-feasibility situation with soft constraints does not mean that the closed-loop system becomes unstable, but that the controller cannot keep the WEC system within the physical limits defined in the Table 4. In addition, in order to obtain a more complete analysis of how this uncertainty affects the closed-loop system, the average powers generated for each value of added uncertainty to each parameter are recorded. A large number of simulations have been carried out for this purpose, all of them using an integration step of 1 ms and the Runge-Kutta method of order 4 (RK4).

Preprints (www.preprints.org) | NOT PEER-REVIEWED | Posted: 28 September 2018 doi:10.20944/preprints201809.0556.v1

Peer-reviewed version available at Energies 2018, 11, 2857; doi:10.3390/en11102857

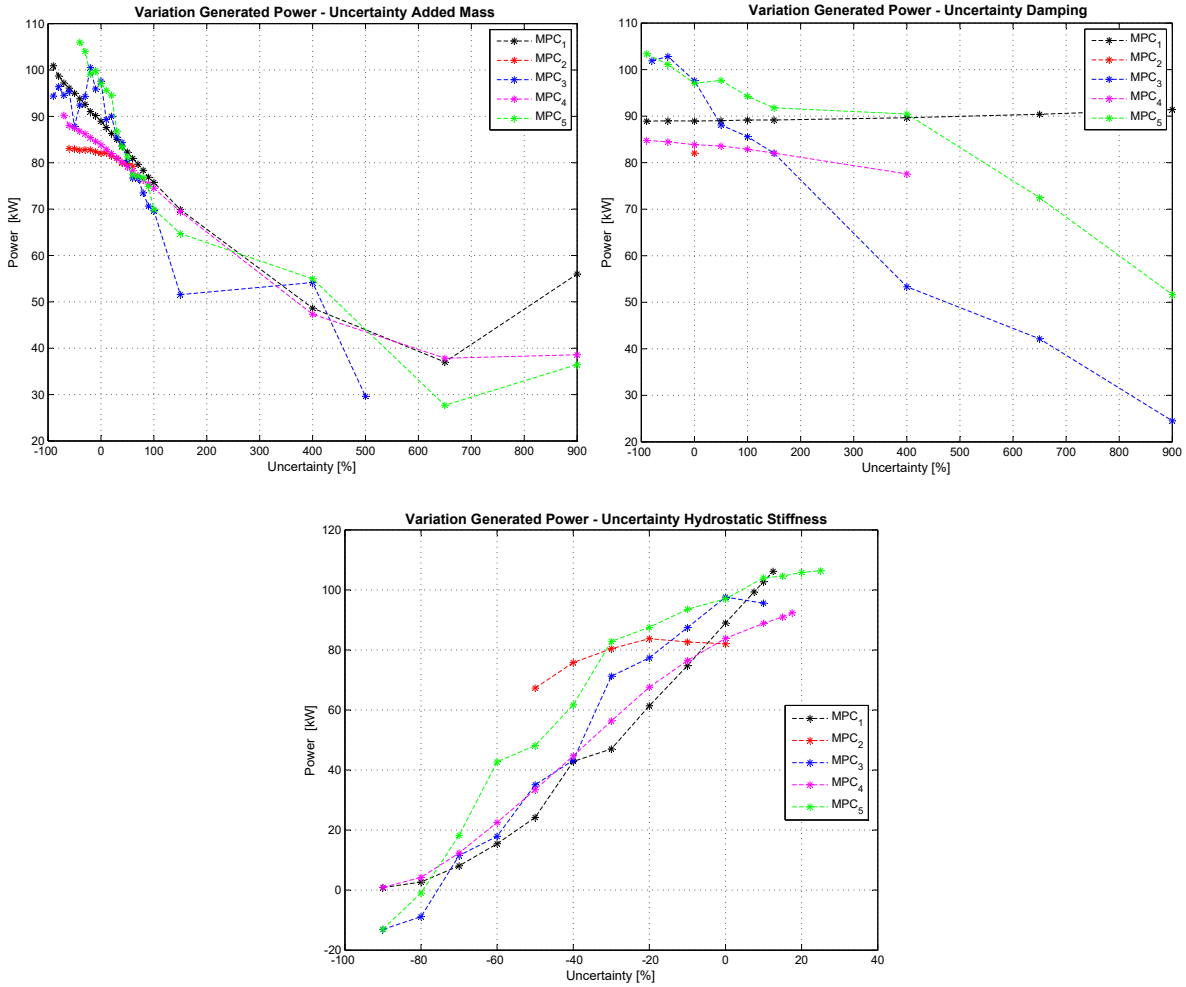

Figure 9. Variations of the average mechanical power generated in function of the added uncertainty to: added mass, damping coefficient and hydrostatic restoring coefficient.

Once the robustness study has been defined, the Figure 9 shows the results obtained in function of the added uncertainties; feasible limits obtained for the five MPCs and the variation of their mean power generated. With respect to the added uncertainty in m_{infty}, the controller MPC_2 is the least robust. Meanwhile, the MPC_1 controller offers the best features in a power-robustness ratio. However, it should be noted that when considering more reasonable added uncertainty values (interval $[-50, 50]\%$), the MPC_5 extracts significantly more power than the others. It should also be noted that the controllers that directly maximize power in their cost function (MPC_1 and MPC_4) have the most predictable behavior with respect to the added uncertainty in m_∞. On the other hand, the MPC_5 offers the best features with respect to the uncertainty added to the dynamics of the radiation force (up to 400%). In contrast, the MPC_2 gives very bad results in this respect. The MPC_1 also gets good results, because it achieves a practically constant power production despite variations of $\triangle_B$. Finally, the Figure 9 shows how the power generated by the different controllers varies according to the uncertainty added to the hydrostatic restoring coefficient of the system. In this aspect, it can be appreciated how the robustness of all the controllers is more limited. Because, if the value of the coefficient k_{res} increases, the excitation force that the wave exerts on the system (51) increases proportionally. Therefore, the margin of action of the PTO system decreases noticeably. Even so, the MPC_5 supports an added uncertainty of 25%, again being the that provides the best robustness results. Note that, for such added uncertainty, the excitation force becomes more than three times the force that the PTO system can apply to the buoy, see Figure 10. After the MPC_5, the MPC_4 and MPC_1 get the best results, in this order.

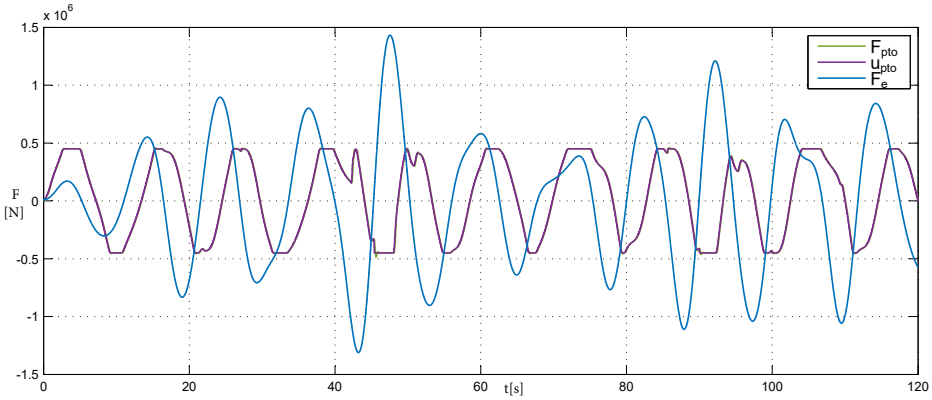

Figure 10. Comparisons between: wave force, force setpoint demanded to the PTO and real force produced by the PTO, by applying in simulation the MPC_5. The model (15) has an added uncertainty to the hydrostatic restoring coefficient of 25%.

5. Conclusions

The interest in implementing MPCs in WECs systems is motivated by the need to increase the productive/economic viability of these systems. For this reason, in this work five different predictive controllers have been designed. All these controllers allow minimizing mechanical fatigue by limiting the operating range of the WEC system by means of hard and soft constraints. The main contribution of this work is the study of performance and robustness carried out for the five MPCs designed. This study demonstrates how the addition of an embedded integrator to the design model improves the performance of the WEC device referring to average power generated, quality of instantaneous power generated, reduction of mechanical fatigue and robustness of the closed-loop system, in comparison with the other MPCs. On the other hand, it has been proven that controllers using design models that consider the dynamics of the PTO system and of the radiation force, obtain instantaneous power peaks lower than those obtained by using simplified models. With respect to the two optimization criteria compared in this paper, it can be concluded that controllers that directly maximize the extracted power get less overshoot of the nominal limits. Whereas controllers that use an optimization criterion based on the minimization of the error between the oscillation speed of the system and a setpoint obtain a higher level of average power extraction. Moreover, in order to provide veracity to this study, in this work an identified methodology for PAWs has been proposed and validated for a scale prototype using experimental time series.

Author Contributions: Rafael Guardeño was responsible for designing the predictive controllers, studying them and writing most of the paper. Agustín Conseglière performed the modeling of the WEC system, proposed the identification methodology for PAW systems and performed its validation. Manuel J. Lopez reviewed all the work done, proposed the comparative robustness and wrote part of the document. Furthermore, Manuel J. Lopez and Agustín Conseglière proposed the control problems to solve using Model Predictive Control strategy.

Acknowledgments: Thanks to all ORPHEO project partners for giving us the opportunity and funds to research in this promising field.

References

1. Pecher. A.; Kofoed, J. P. *Handbook of Ocean Wave Energy*, Sprinder Open, Boca Raton, USA, 2016, ISBN 978-3-319-39888-4.
2. The Ocean Energy Systems Technology Collaboration Programme, Available online: www.ocean-energy-systems.org/index.php (accessed on 4 may 2017).
3. Pelagic Power, Available online: www.pelagicpower.no/about.html (accessed on 6 may 2017).
4. Falnes, J. *Ocean Waves and Oscillating Systems*, Cambridge University Press, New York, USA, 2002, ISBN 0-521-78211-2.

5. Drew, B.; Plummer, A. R.; Sahinkaya, M. N. A review of wave energy converter technology, *J. Power Energy*, **2009**, *223*, 887-902, doi: 10.1243/09576509JPE782.
6. Valério, D.; Beirao, P.; Mendes, M. J. G. C.; Costa, J. S. da. Comparison of control strategies performance for a Wave Energy Converter. In *16th Mediterranean Conference on Control and Automation*; 2008; ; pp. 773–778.
7. Li, G. Predictive control of a wave energy converter with wave prediction using differential flatness. In *Proceeding of the 54th IEEE Conference on Decision and Control*; 2015; pp. 3230–3235.
8. Andersen, P.; Pedersen, T. S.; Nielsen, K. M.; Vidal, E. Model Predictive Control of a Wave Energy Converter. In *IEEE Conference on Control Applications*; 2015; pp. 1540–1545.
9. Brekken, T. K. On Model Predictive Control for a point absorber Wave Energy Converter. In *IEEE Trondheim PowerTech*; 2011; pp. 1–8.
10. Richter, M.; Magana, M. E.; Sawodny, O.; Brekken, T. K. a Nonlinear Model Predictive Control of a Point Absorber Wave Energy Converter. *IEEE Trans. Sustain. Energy*, **2013**, *4*, 118-126, doi: 10.1109/TSTE.2012.2202929.
11. G. Li; M. R. Belmont, Model predictive control of sea wave energy converters - Part I: A convex approach for the case of a single device, *Renew. Energy*, **2014**, *69*, 453-463, doi: 10.1016/j.renene.2014.03.070.
12. Cavaglieri, D.; Bewley, T. R.; Previsic, M. Model Predictive Control leveraging Ensemble Kalman forecasting for optimal power take-off in wave energy conversion systems. In *Proceedings of the American Control Conference*; 2015; Vol. 2015–July, pp. 5224–5230.
13. Oetinger, D.; Magaña, M. E.; Member, S.; Sawodny, O. Decentralized Model Predictive Control for Wave Energy Converter Arrays. *Sustain. Energy, IEEE Trans.* **2014**, *5*, 1099–1107, doi:10.1109/TSTE.2014.2330824.
14. Li, G.; Belmont, M. R. Model predictive control of a sea wave energy converter: A convex approach. In *The International Federation of Automatic Control*; IFAC, 2014; Vol. 19, pp. 11987–11992.
15. Soltani, M. N.; Sichani, M. T.; Mirzaei, M. Model Predictive Control of Buoy Type Wave Energy Converter. In *The International Federation of Automatic Control*; IFAC, 2014; Vol. 47, pp. 11159–11164.
16. Starrett, M.; So, R.; Brekken, T. K. A.; McCall, A. Increasing power capture from multibody wave energy conversion systems using model predictive control. In *Technologies for Sustainability*; 2015; pp. 20–26.
17. Lagoun, M. S.; Benalia, A.; Benbouzid, M. E. H. A predictive power control of Doubly fed induction generator for wave energy converter in irregular waves. In *1st International Conference on Green Energy*; 2014; pp. 26–31.
18. Camacho, E.F; BordonsC. *Model Predictive Control*, Sprinder, Sevilla, Spain, ISBN 978-1-85233-694-3.
19. Wang, L. *Model Predictive Control System Desing and Implementation Using MATLAB*, Sprinder, Melbourne, Australia, 2009, ISBN 978-1-84882-330-3.
20. Bozzi, S.; Miquel, A. M.; Antonini, A.; Passoni, G.; Archetti R. Modeling of a point absorber for energy conversion in Italian seas, *Energies* **2013**, *6*, 3033–3051, doi:10.3390/en6063033.
21. Hong, Y.; Eriksson, M.; Boström, C.; Waters, R. Impact of generator stroke length on energy production for a direct drivewave energy converter. *Energies* **2016**, *9*, 1–12, doi:10.3390/en9090730.
22. Hansen, R. H.; Kramer, M. M. Modelling and Control of the Wavestar Prototype. In *Proceedings of the 9th European Wave and Tidal Energy Conference*; 2011; pp. 1–10.
23. Kovaltchouk, T.; Multon, B.; BenAhmed, H.; Glumineau, A.; Aubry, J. Influence of control strategy on the global efficiency of a Direct Wave Energy Converter with electric Power Take-Off. In *Eighth International Conference and Exhibition on Ecological Vehicles and Renewable Energies*; 2013; pp. 1–10.
24. Fusco, F.; Ringwood, J. V A study of the prediction requirements in real-time control of wave energy converters. *IEEE Trans. Sustain. Energy*, **2012**, *3*, 176 - 184, doi: 10.1109/TSTE.2011.2170226.
25. Tedeschi, E.; Carraro, M.; Molinas, M.; Mattavelli, P. Effect of control strategies and power take-off efficiency on the power capture from sea waves. *IEEE Trans. Energy Convers.*, **2011**, *26*, 1088-1098, doi: 10.1109/TEC.2011.2164798.
26. Cummins W., The Impulse Response Function and Ship Motions, *Schiffstechnick*, **1962**, *9*, 101-109, doi: 39080027544292.
27. Brandtsegg I., Validation of a Combined Wind and Wave Power Installation, Master, Norwegian University of Science and Technology, Norway, 2014.
28. Openore, Available online: https://openore.org/2016/04/28/openwec/ (accessed on 14 may 2017).
29. Falnes, J. *Ocean Waves and Oscillating Systems*, Cambridge University Press, New York, USA, 2002, ISBN 0-521-78211-2.
30. Parks, T. W.; Burrus, C. S. *Digital Filter Design*, Wiley, Michigan, USA, 1987, ISBN 9780471828969.

462 31. Morison, J.R.; O'Brien M.P.; Johnson, J.W.; Schaaf, S.A. The forces exerted by surface waves on piles, *Society*
463 *of Petroleum Engineers* **1950**, *189*, 149-154, doi:10.2118/950149-G.
464 32. Ogata K. *Ingeniería de control moderna*, PEARSON EDUCACIÓN S.A., Madrid, Spain, 2010, ISBN
465 9788483226605.
466 33. Mathworks, Available online: https://es.mathworks.com/help/optim/ug/quadprog.html (accessed on 17
467 may 2017).